Developmental Biology **212,** 465–476 (1999)
Article ID dbio.1999.9349, available online at http://www.idealibrary.com on IDEAL®

Domain 20 Reveals That the Larval Visual System Is Derived from a Subdomain of a Few Cells

Ruria Namba[1] and Jonathan S. Minden[2]

Department of Biological Sciences and Center for Light Microscope Imaging and Biotechnology, Carnegie Mellon University, Pittsburgh, Pennsylvania 15213

In an attempt to study the fates of cells in the dorsal head region of *Drosophila* embryos at gastrulation, we used the photoactivated gene expression system to mark small numbers of cells in selected mitotic domains. We found that mitotic domain 20, which is a cluster of approximately 30 cells on the dorsal posterior surface, gives rise to various ectodermal cell types in the head, including dorsal pouch epithelium, the optic lobe, and head sensory organs, including Bolwig's organ, the larval photoreceptor organ. We found that the optic lobe and larval photoreceptors share the same origin of a few adjacent cells near the center of mitotic domain 20, suggesting that within the mitotic domain, there is a subdomain from which the larval visual system is specified. In addition to the components of the larval visual system, this central region of mitotic domain 20 also generates a part of the eye–antennal disc placode; cells that gives rise to the adult visual system. We also observed that a significant amount of cell death occurred within this domain and used cell ablation experiments to determine the ability of the embryo to compensate for cell loss. © 1999 Academic Press

***Key Words: Drosophila;* fate map; mitotic domain; larval visual system; β-galactosidase; ricinA; p35.**

INTRODUCTION

Development of the Larval Visual System

Unlike the complex adult visual system, the larval visual system in *Drosophila* is composed of a set of fairly small photoreceptor organs located bilaterally inside the larval head (Zipursky *et al.*, 1984; Steller *et al.*, 1987). This photoreceptor organ, called Bolwig's organ, consists of 12 photoreceptor cells and sits in the dorsal pouch epithelium. Each photoreceptor extends an axon that fasciculates to form the Bolwig's nerve which projects posteriorly toward the optic lobe, the target of the adult visual system on the posterior ventral part of the brain, and establishes connections with target cells in the brain.

The differentiation and development of the larval visual system have been described previously using cell-type-specific markers (Schmucker *et al.*, 1992, 1997; Green *et al.*, 1993). Although they are separate in their final position, the optic lobe and Bolwig's organ derive from the same area in the posterior dorsolateral region of the embryonic head at stage 12 (Green *et al.*, 1993). Genetically, they are distinguished by their FasII expression at stage 12 (Hartenstein and Campos-Ortega, 1985); a subset of the FasII-positive cells expresses *Kruppel* as a photoreceptor-specific marker and the rest express *disconnected* (*disco*), which is an optic lobe-specific marker (Schmucker *et al.*, 1992, 1997; Cheyette *et al.*, 1994). At stage 11, the optic lobe precursors can be recruited to become neighboring photoreceptor cells by inhibiting the function of PATCHED, further supporting that these two cell types share a common origin (Schmucker *et al.*, 1994). Between stages 12 and 13, the optic lobe invaginates from the head epithelium, while photoreceptor precursors stay within the epithelium and form a distinct cluster of polarized cells. Initially, 4 to 6 photoreceptors differentiate, but by stage 14 all 12 cells create a complete Bolwig's organ (Schmucker *et al.*, 1992). Also during this stage, Bolwig's organ precursor cells extend their axons to the optic lobe. During head involution, the Bolwig's organ moves anteriorly away from the optic lobe.

[1] Current address: Section of Molecular and Cellular Biology, University of California, Briggs Hall, Davis, CA 95616.
[2] To whom correspondence should be addressed. Fax: (412) 268-7129. E-mail: minden@cmu.edu.

0012-1606/99 $30.00

Relationship of the Larval and Adult Visual Systems

The developmental processes of the adult and the larval visual systems have several overlapping features. The larval visual system has the same basic composition as the adult visual system with photoreceptor axons projecting to their targets through the optic stalk in a stereotypical pathway (Zipursky *et al.*, 1984; Steller *et al.*, 1987; Schmucker *et al.*, 1997). The adult visual system develops in close proximity to the larval visual system. Adult eyes develop from the eye imaginal discs starting from the third-instar larval stage (Meinertzhagen and Hanson, 1993). The eye imaginal disc derives as a part of the eye–antennal disc, which invaginates as two pouches from the posterior part of the larval dorsal pouch (Younossi-Hartenstein *et al.*, 1993). The eye–antennal disc develops above the path of the Bolwig's nerve and in the third-instar larvae, the Bolwig's nerve is found projecting through the eye imaginal disc (Tix *et al.*, 1989). The target of adult photoreceptors, the optic lobe, is also adjacent to the target of the Bolwig's nerve in the brain (Campos *et al.*, 1995). Differentiated photoreceptor axons extend from the eye imaginal disc through the optic stalk and project along the Bolwig's nerve path to establish a connection with the optic lobe.

Many of the genes involved in adult visual system development have similar roles in larval visual system differentiation. *eyeless*, the master regulator of eye development, is expressed in photoreceptor cells at stage 12 and then in the entire larval visual system as well as in a part of the brain and eye–antennal disc at the end of embryogenesis (Halder *et al.*, 1995; Sheng *et al.*, 1997). Another adult eye-development regulator, *sine oculis* (*so*), is also important for larval visual system development (Heitzler *et al.*, 1993; Serikaku and O'Tousa, 1994). *so* is expressed as early as stage 5 in the dorsal region anterior to the cephalic furrow (Cheyette *et al.*, 1994; Serikaku and O'Tousa, 1994).

Various fate mapping studies have suggested that the adult and larval visual systems derive from the same region in the embryo. The optic lobe was mapped to the dorsal posterior head region of the gastrulating embryo (Hartenstein *et al.*, 1985). Green *et al.* (1993) showed that the Bolwig's organ originates from a part of the optic lobe invagination in the dorsal lateral head region of stage 12 embryos by using BrdU labeling and various cell-type-specific marker studies. The adult eye placode was mapped to a region in the dorsal posterior head of the blastoderm by gynandomorph mapping (Struhl, 1981). From cell ablation experiments, the origin of the eye–antennal disc was indirectly mapped to the dorsal lateral part of the embryonic head (Jurgens *et al.*, 1986). Analysis of enhancer trap lines showed that the eye–antennal disc develops from a large area spanning multiple head segments (Younossi-Hartenstein *et al.*, 1993). The origin of the eye–antennal disc placode, however, has not been mapped directly to the gastrulating embryo.

We have used the photoactivated gene expression system (Cambridge *et al.*, 1997) to study cell fates of gastrulation-stage embryos. Light-sensitive, caged GAL4VP16 was injected into blastoderm-stage embryos and *UAS-lacZ* was expressed ectopically by uncaging GAL4VP16 protein with UV irradiation of a small area of the embryos at gastrulation The first zygotically regulated cell divisions in *Drosophila* embryos occur in a distinct and reproducible pattern at the beginning of gastrulation (Foe, 1989). Synchronously dividing groups of cells, mitotic domains, have been shown to represent cell fate domains (Cambridge *et al.*, 1997). Here, we show that cells in mitotic domain 20 on the dorsal posterior surface of the embryonic head give rise to various head ectodermal structures including the larval visual system. By marking a small group of cells at gastrulation, we found that in the center of mitotic domain 20, there is a group of three to four cells whose fate is restricted to the Bolwig's organ and optic lobe. Moreover, a part of the eye–antennal disc appears to originate from these cells.

MATERIALS AND METHODS

Fly Stocks

The following stocks were used: *UAS-lacZ* on the X chromosome (N. Perrimon), *UAS-p35* on the third chromosome (B. Hay), *UAS-ricinA/CyO* (A. Brand), and *Ubi-GFPnls* and *H99/TM3* (both from Bloomington stock center). *UAS-lacZ; H99* and *UAS-lacZ; UAS-p35* lines were created from the above stocks.

Development of the *UAS-lacZ* embryos was normal with respect to viability and cell death patterns. The latter was monitored by acridine orange injection as described previously (Namba *et al.*, 1997). The viability of *UAS-p35* embryos was also normal. Injection of caged GAL4VP16 at 17 μg/ml did not affect the viability of embryos from these stocks.

Antibodies

The following antibodies were used in combination with biotin-conjugated secondary antibodies (1:2000; Vector Laboratories) according to the specified dilution: monoclonal mouse anti-β-galactosidase (1:1500; Sigma), rabbit anti-β-galactosidase (1:2000; Cappel), monoclonal mouse 22C10 (1:10; J. Pollock), mouse anti-FasII (1:20; Corey Goodman), and rat anti-escargot (1:1000; S. Hayashi).

Embryo Preparation

Embryos were collected on apple juice agar plates with a small bead of yeast paste and subsequently dechorionated in 50% bleach for 2 min. Dechorionated embryos were lined up on a 2.25% agar block and transferred to a coverslip with an adhesive made from heptane-dissolved double-sided tape on which they were aligned in the desired orientation using forceps (for dorsal activation, the dorsal surface faced down on the coverslip). For injection, embryos were desiccated over Drierite and covered with halocarbon oil (series 700; Halocarbon Products Corp., River Edge, NJ). Images of mitotic domains in Ubi-GFPnls embryos were collected on a confocal microscope (MRC 600; Bio-Rad). Photoactivation and DIC imaging were performed on an inverted microscope (IX70; Olympus).

Photoactivated Gene Expression

Caged GAL4VP16 was prepared as previously described (Cambridge *et al.,* 1997). The optimal dilution of caged GAL4VP16 was determined empirically by photoactivating embryos with varying amounts of caged GAL4VP16 and assaying for the efficiency of uncaging and the effect on embryonic development. Photoactivation of *UAS-lacZ* embryos injected with 17.8 μg/ml caged GAL4VP16 had no effect on development and the concentration resulted in good *lacZ* expression as assayed by X-gal staining and was used for all experiments in this paper. Embryos were injected near the site of future activation and usually kept at 18°C until activation. Embryos that leaked were disregarded.

The length of activation varied depending on the width of the activation beam. Using a 60× objective lens, embryos were irradiated for 15 s to activate a single cell. For a larger beam size (4–15 cells), the irradiation time was decreased to 10 s. After the activation, the embryos were kept on the coverslip under halocarbon oil at 18°C or room temperature and fixed at the desired stage. For a given photoactivation session, approximately 50 embryos were activated.

Visualization of Marked Cells

To fix the embryos, the halocarbon oil was removed as completely as possible by scraping. The embryos and residual oil were gently washed off the coverslip with heptane in a small petri dish. The embryos were transferred to an 8-ml glass, screw-cap tube and washed thoroughly with several changes of heptane to remove any dissolved oil and glue. Fixation of photoactivated embryos was done essentially as described by Vincent and O'Farrell (1992). Briefly, the embryos were fixed in 1:1 heptane:11% formaldehyde in PBS by gently rocking for 30 min. The embryos were transferred onto a Nytex membrane covering the opening of a 15-ml Falcon tube and heptane was blotted by applying Kimwipes from the other side. Dried embryos were immediately stamped onto double-stick tape and covered with PBS for hand devitellinization. The embryos were devitellinized by gently pushing the posterior end with forceps. These devitellinized embryos in PBS were washed several times in methanol before starting the antibody staining. The embryos were stable for several days in ethanol at −20°C.

Antibody staining was done essentially as described by Cambridge *et al.* (1997). Staining was typically done in a 200-μl volume in a 1.5-ml microfuge tube. Primary and secondary antibodies were incubated without rotation for 2–18 h at room temperature. The efficiency of antibody staining of the photoactivated embryos varied depending on the number of cells being activated. The larger the area of activation, the more embryos showed labeling. For 4- to 12-cell activation experiments, the average labeling efficiency was about 50%, sometimes as high as 90%.

Histochemical detection of biotinylated secondary antibodies was performed with Vectastain Elite ABC kit (Vector Laboratories). The presence of antigen was detected by the peroxidase reaction with 0.5 mg/ml diaminobenzidine tetrahydrochloride. To detect two different antigens, after the first reaction was done with the biotinylated secondary antibody, the second color reaction was carried out on the dehydrated embryos in the presence of 0.3% cobalt chloride. These embryos were mounted in 1:1 Canada balsam:methylsalicylate.

RESULTS

Development of Mitotic Domain 20

Mitotic domain 20 (hereafter referred to as δ20) is the most posterior of the three dorsal head mitotic domains consisting of roughly 30 cells at interphase of nuclear cycle 14 (Fig. 1A). A small number of cells within δ20 were marked at stage 8 (Campos-Ortega and Hartenstein, 1985), when the nuclear cycle 14 mitotic domains first appear, by activating *UAS-lacZ* expression using the photoactivated gene expression system (Cambridge *et al.*, 1997). Since the cells in δ20 divide much later than surrounding mitotic domains and most of the cells divide inside the cephalic furrow as suggested by Foe (1989), it was difficult to distinguish δ20 cells as they divide. Therefore, δ20 cells, identified as those cells surrounded by the amnioserosa and mitotic domains 5, 18, and B, were photoactivated before δ20 entered mitosis (Fig. 1A, green circle). The fates of these cells were determined at the end of embryogenesis by detecting the presence of β-galactosidase.

Photoactivation of approximately 12 cells in the center of δ20 gave rise to a set of bilaterally symmetrical structures spanning from the anterior tip to the brain (Fig. 1B), including many head sensory organs and nerves of the peripheral nervous system (PNS), the posterior part of the brain, and the dorsal pouch epithelium above the clypeolabrum. Activation of δ20 cells also gave rise to a significant amount of cellular debris, indicating that some cells were dying. Previous studies showed that the photoactivation procedure does not affect cell death patterns (Cambridge *et al.*, 1997). The whole-mount *in situ* antibody staining method used here could not reveal the exact time of cell death since the β-galactosidase within the cellular debris persisted even after phagocytosis by macrophages.

Cells in the mitotic domains adjacent to δ20 were marked to determine if there was any overlap of fates with δ20. Cells in δ18, which defines the anterior border of δ20, mainly gave rise to the dorsal pouch epithelia that did not overlap with the dorsal pouch cells derived from δ20 (Fig. 1C). δ5 is a paired domain that demarcates the lateral borders of δ20. Although the progeny of δ5 cells were sparsely distributed at the anterior tip, at the dorsal pouch, and possibly in the brain, this pattern was very different from δ20. The δ20-derived PNS nerves connecting the anterior tip to the brain were not observed in marked δ5 cells (Fig. 1D). δB is situated laterally to δ20 and anterior to δ5. Photoactivated δB cells populated the central part of the central nervous system (CNS) and the anterior tip of the embryo (Fig. 1E). None of these cells became part of the dorsal pouch as was the case for δ18 and δ20. These data show that δ20 produces cellular fates that are distinct from its neighboring mitotic domains.

δ20 starts as a single domain on the dorsal midline. During germ band extension, the cells of δ20 moved bilat-

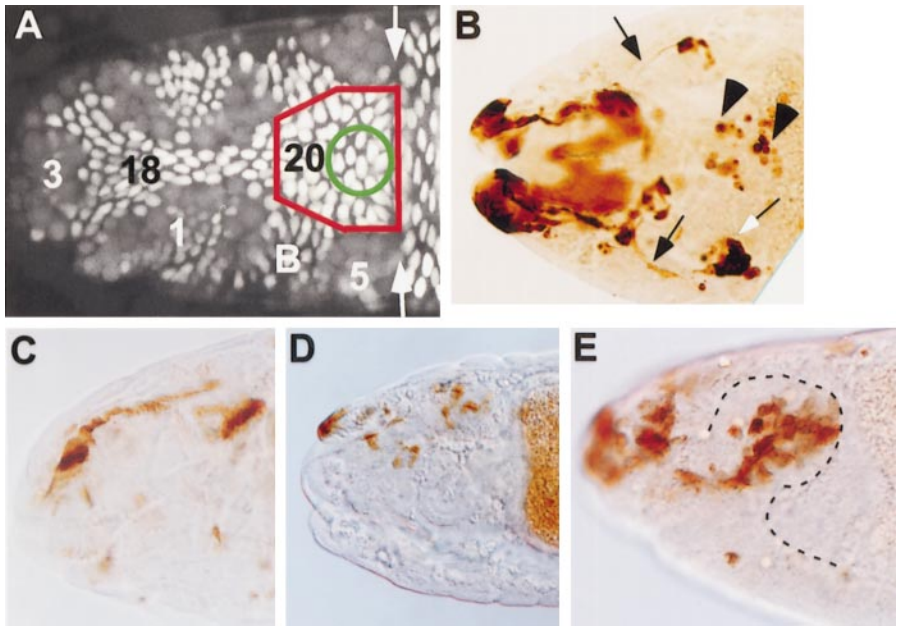

FIG. 1. Fate mapping of the dorsal head mitotic domains. (A) Individual cells of the dorsal head mitotic domains were visualized by the expression of nuclear GFP (*Ubi-GFPnls*) by confocal microscopy. δ20 is highlighted with a red border. The numbers indicate mitotic domains. Interphase nuclei appear bright and have sharp edges while mitotic cells are large and appear diffuse. The white arrows point to the cephalic furrow. The green circle indicates a typical size and location of the UV photoactivation beam. All embryos are shown with anterior to the left. (B to E) Fates of mitotic domains were visualized by GAL4-dependent activation of *lacZ* using the photoactivated gene expression system. (B) Dorsal view of a stage 17 embryo with photoactivated δ20 cells. Cells in the posterior part of the brain (white arrow) and head PNS (including axons projecting to the brain; arrows) were marked as well as cellular debris (arrowheads). (C) Lateral view of a stage 17 embryo with photoactivated δ18 cells in the dorsal pouch. (D) Dorsal view of a stage 17 embryo with photoactivated δ5 cells at the anterior tip and in the brain. (E) Lateral view of a stage 15 embryo with photoactivated δB cells at the anterior tip and in CNS (outlined with a dotted line).

erally away from the dorsal midline (Fig. 2A). By 2 h after photoactivation at stage 7, most δ20 cells had migrated laterally away from the dorsal midline where they formed the dorsal border of the gnathal segments (Fig. 2B). At late stage 11, the first sign of cell death was apparent by punctate staining of cell debris spreading posteriorly away from the marked δ20 cells. This corresponded to the stage and location of the first appearance of embryonic cell death (Abrams *et al.*, 1993). By the end of stage 13, the cells formed a narrow strip spanning from the ventral to the dorsal surface (Fig. 2C). At the end of embryogenesis, cells in this narrow strip were distributed into three clusters spanning the entire length of the head (Fig. 2E). The ventral δ20 cells moved anteriorly with the invagination of the gnathal segments through the stomodeal invagination (Fig. 2D) and eventually reached the anterior tip. The more dorsal δ20 cells formed the dorsal ridge and became a part of the dorsal pouch, while some cells delaminated and occupied the ventral posterior part of the brain lobe. The cells in the brain lobe were usually connected to a cell cluster in the anterior tip of the embryo by long nerve-like projections (Fig. 2E, arrow).

Identifying the Larval Visual System within the Structures Deriving from δ20

Photoactivation of δ20 marked a pair of lateral clusters of cells in the dorsal pouch adjacent to the pharynx in the stage 16 embryo (Fig. 3A). This cluster projected a nerve to the posterior part of the brain and the entire projection path was marked by the *lacZ* expression. The location and morphology of this structure suggested that it was the larval photoreceptor organ, Bolwig's organ. In order to confirm that the Bolwig's organ derived from δ20, the expression of a PNS-specific marker was visualized in δ20-photoactivated embryos. The monoclonal antibody 22C10 was used to highlight the entire PNS, including sensory organs and their axons (Fujita *et al.*, 1982; Goodman *et al.*, 1984). Double staining δ20-activated embryos for β-galactosidase expression and with mAb 22C10 showed that the photoactivated δ20 cells coincided with the Bolwig's organ, fasciculated axons of the Bolwig's organ (Bolwig's nerve), and cells at the termini of Bolwig's nerve presumably in the optic lobe (Fig. 3B).

In addition to producing the larval visual system, some δ20 cells were observed to form an epithelium on top of the

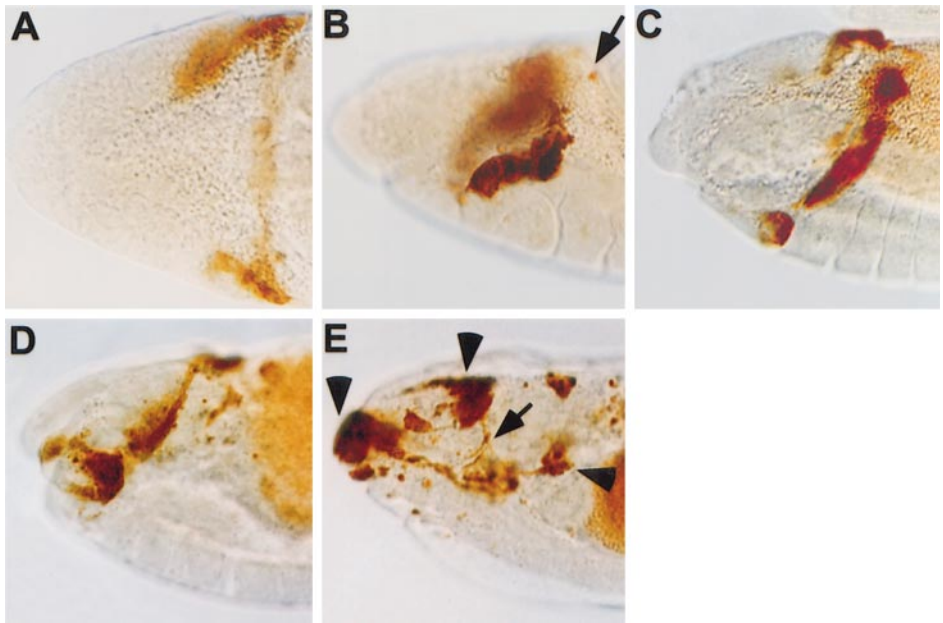

FIG. 2. Development of δ20. Dorsal (A) and lateral (B to E) images of δ20-photoactivated embryos. The marked cells were visualized with an anti-β-galactosidase antibody. (A) The cells in δ20 moved away from the dorsal midline during germ band extension. (B) At late stage 11, the cells reached the dorsal border of the gnathal segments. The first sign of cell death was apparent as a small spot moving away from the group of marked cells (arrow). (C) At stage 13, the marked δ20 cells extended along the lateral surface. (D) During stage 14, the ventral cells continued to move anteriorly into the stomodeal invagination. (E) At the end of embryogenesis, cells were distributed into three clusters (arrowheads): the anterior tip, the dorsal pouch, and the brain, connected via nerve-like projections (arrow).

Bolwig's nerve projection path (Fig. 3, white arrows). The Bolwig's nerve extends posteriorly from the Bolwig's organ located inside the dorsal pouch epithelium and makes a sharp, ventral turn near the posterior edge of the dorsal pouch to follow along the basal surface of the brain into the optic lobe. The δ20 cells that formed the epithelial structure were often found at or near where the Bolwig's nerve made the ventral turn. This roughly corresponds to the location of the eye–antennal disc placode. The eye–antennal disc placode is located in the posterior part of the dorsal pouch as seen by the expression of *escargot* (*esg*) in a V-shaped pattern (Fuse *et al.*, 1996; Fig. 3C). Double labeling of δ20 cells with an anti-*esg* antibody showed partial overlap of δ20 cells with *esg*-expressing cells in the dorsal pouch especially at the anterior part of the V-shaped placode (Fig. 3D).

Single-Cell Labeling of δ20 Highlights the Development of the Larval Visual System

In order to determine the range of fates from single δ20 cells, the photoactivation beam was narrowed to less than 1 cell diameter, about 4 μm. Photoactivation of a single cell in the center of δ20 typically marked the larval visual system either on the left- or on the right-hand side of the embryo, while a small fraction of these embryos had marked, visual system cells on both sides of the embryo midline (Fig. 4C). Green *et al.* (1993) observed that the cells in the presumptive optic lobe region (including future photoreceptors) undergo four postblastoderm mitoses before they invaginate. Therefore, one expects that a single δ20 cell should give rise to 16 progeny cells by the end of stage 11. We typically observed between 12 and 15 marked cells in embryos that were aged to stage 14–16. The fewer than 16 marked cells can be accounted for by the death of a fraction of the photoactivated cell's progeny. It is possible that the UV beam activated more than 1 cell, but this is unlikely judging from the number of cells labeled and the high frequency of observing the same pattern of marked cells. It was difficult to assess the frequency of successful photoactivation for the following reasons: (1) not all embryos were photoactivated because of their developmental stage or orientation, (2) variability in the injected volume of caged GAL4VP16—some embryos received too little caged GAL4VP16, and (3) a fraction of the embryos were lost or damaged during the staining procedure. We estimate that the frequency of photoactivation of an area containing 4–15 cells was usually 50–75%, while the frequency of single-cell photoactivation was 10–15%.

Although various structures in addition to the larval visual system derive from δ20, photoactivation of single cells in the center of the mitotic domain gave rise to marked cells in the optic lobe, the Bolwig's organ, and a small area of the dorsal pouch, presumably the eye–

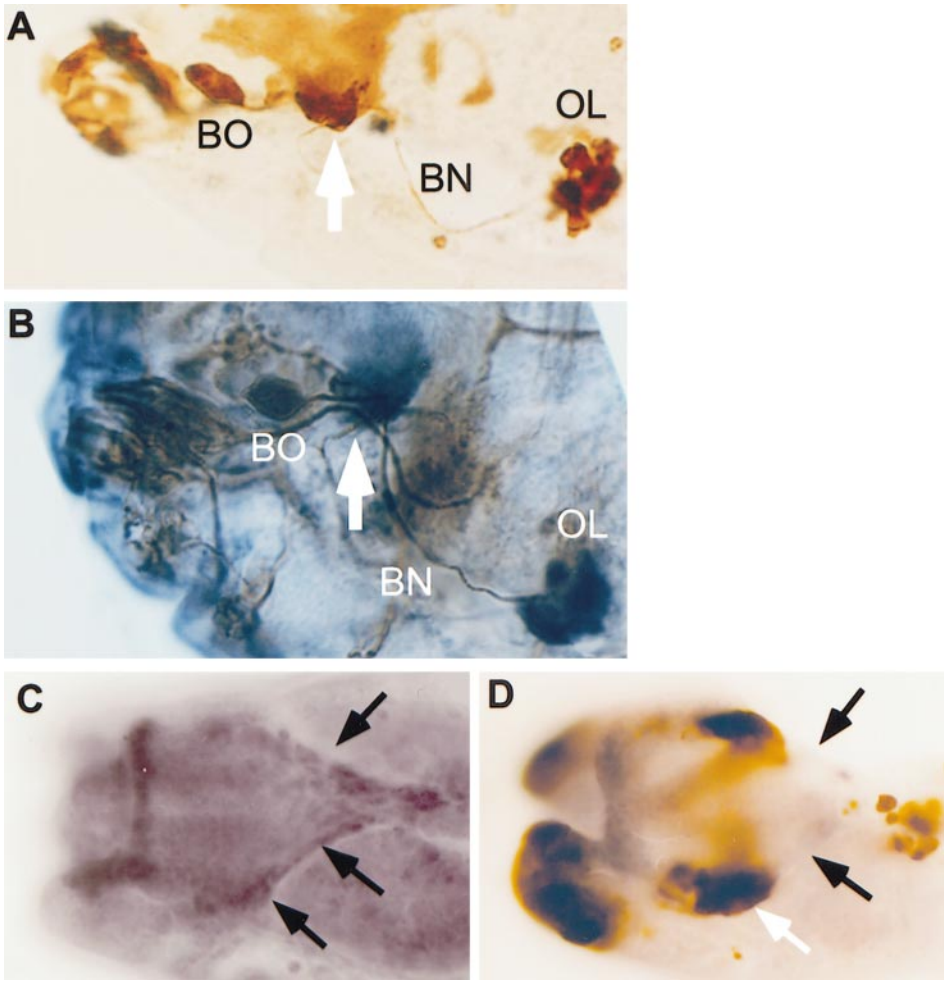

FIG. 3. δ20 generates the larval visual system. (A and B) Dorsal view of δ20-marked embryos. (A) β-Galactosidase was expressed in the Bolwig's organ (BO), the Bolwig's nerve (BN), and the optic lobe (OL). White arrows point to cells in the dorsal pouch on top of the Bolwig's nerve path. (B) β-Galactosidase expression (blue) in the larval visual system overlaps with PNS marker expression as visualized with mAb 22C10 (brown). (C) Dorsal view of a stage 16 embryo labeled with anti-ESG. ESG, an imaginal disc marker, is expressed in a V-shaped pattern in the posterior part of the dorsal pouch (black arrows). (D) Dorsal view of a stage 16 embryo photoactivated in δ20. This embryo was labeled with anti-β-galactosidase (brown) and anti-ESG (blue) antibodies. The V-shaped ESG expression pattern (black arrows) overlapped partially with the marked δ20 cells at the anterior tip (white arrow).

antennal disc placode, exclusively (Figs. 4A and 4B). Before head involution, these dorsal pouch cells were found adjacent to the photoreceptor cells (Fig. 4A, arrow) and by the end of embryogenesis, the labeled cells were usually near where the Bolwig's nerve made the ventral turn, correlating to the presumptive site of the eye–antennal disc (Fig. 4B, arrow). The entire larval visual system, however, was certainly derived from more than 1 cell in δ20 since single-cell photoactivation yielded smaller areas of marked optic lobe and Bolwig's organ compared to the marked regions resulting from 12-cell photoactivation experiments (compare Figs. 3A and 4). Sixteen, single-cell-photoactivated embryos that were in the correct orientation for analysis were scored (Table 1). Despite the small sample size, there was a clear bias in the pattern of marked cells. All embryos had marked optic lobe cells. About 30% of the embryos had marked optic cells only (Fig. 4C), about 10% had marked optic lobe plus dorsal pouch (Fig. 4D) or Bolwig's organ (Fig. 4E), and the rest (~45%) had all three cell types marked. There were no examples of exclusively marked Bolwig's organ and/or dorsal pouch epithelia, without optic lobe. This suggests that Bolwig's organ and eye–antennal disc precursors are derived from optic lobe progenitors. Several embryos had marked cells on either side of the dorsal midline, indicating that there was no left–right restriction to the migration of midline cells (Fig. 4C).

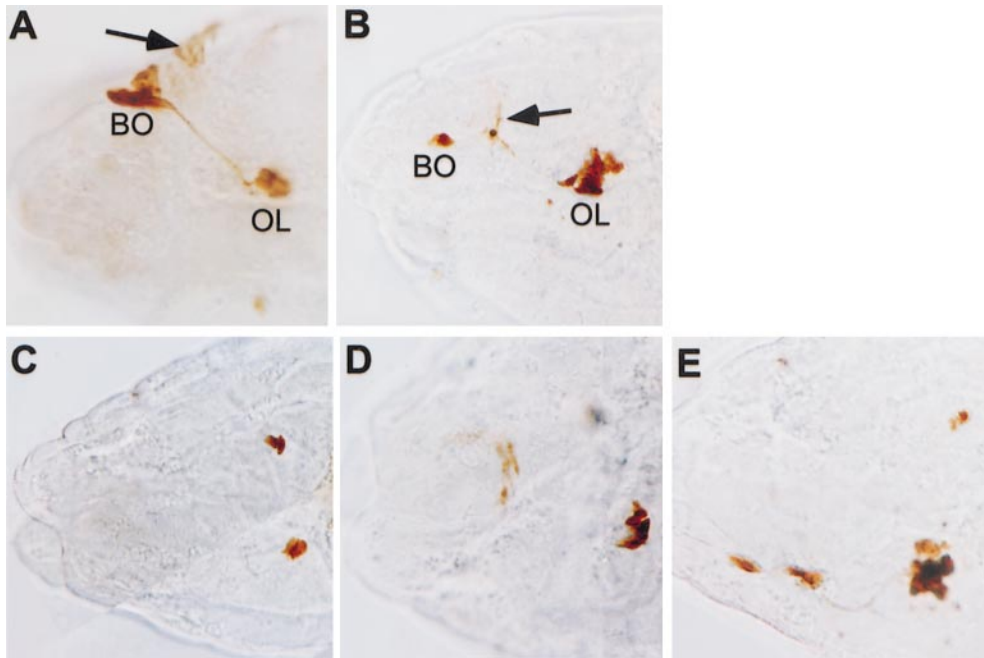

FIG. 4. Single-cell photoactivation of δ20. In embryos from single-cell photoactivation of δ20, marked cells were found in the developing larval visual system at stage 14 (A) and at stage 17 (B), both lateral views. They were confined to the Bolwig's organ (BO), the optic lobe (OL), and the dorsal pouch (arrows). (C) A dorsal view of an embryo with marked cells in both optic lobes. (D) A dorsal view of an embryo with marked cells in the optic lobe and the dorsal pouch. (E) A dorsal view of an embryo with marked cells in the photoreceptor cells and both optic lobes. In order to show all marked cells, images from multiple focal planes were combined.

Cell Ablation with RicinA

Selected cells can be ablated in a cell-autonomous manner by photoactivating the expression of *UAS-ricinA*. RicinA is a protein synthesis inhibitor that has been used to study neuronal development in *Drosophila* embryos (Endo and Tsuguri, 1988; Moffat *et al.*, 1992; Hidalgo *et al.*, 1995; Hidalgo and Brand, 1997). Ablation of four to six cells in δ20 often caused developmental defects in the larval visual system as revealed by staining with anti-FasII and mAb 22C10 antibodies (Fig. 5). FasII is expressed in the Bolwig's organ, Bolwig's nerve, and optic lobe (Fig. 5A); mAb 22C10 highlights the Bolwig's organ and nerve. Since the exact location of the larval visual system placode within δ20 was not known, random activation of ricinA often caused defects in several δ20-derived structures and there was a significant reduction in embryo viability. The most common defect in the larval visual system was found in the Bolwig's organ. In many embryos, one or both Bolwig's organs had an abnormal shape (Figs. 5C–5E). These photoreceptor cells failed to compact into a nice rosette shape and sometimes seemed to have fewer than the normal number of cells (Fig. 5D). Regardless of its abnormal shape, most of the Bolwig's organ extended the Bolwig's nerve toward the optic lobe, although some optic lobes seemed smaller than normal (Fig. 5E). A few embryos had truncated Bolwig's nerves and were missing the corresponding optic lobe (Figs. 5C and 5D); others were missing one side of the larval visual system (Fig. 5B). We did not find any embryos missing optic lobes or Bolwig's organs on both sides.

TABLE 1

Structures Arising from Single-Cell Photoactivation in the Center of δ20

Optic lobe	+			+	+		+
Bolwig's organ		+		+		+	+
Eye disc			+		+	+	+
Occurrences	5	0	0	2	2	0	7

Larval Visual System Development in Cell Death-Deficient Embryos

The appearance of cellular debris arising from photoactivated δ20 cells suggested many of these cells died between stages 11 and 17. The lack of cell death is known to cause general morphological defects in head development as seen in the head involution-defective phenotype

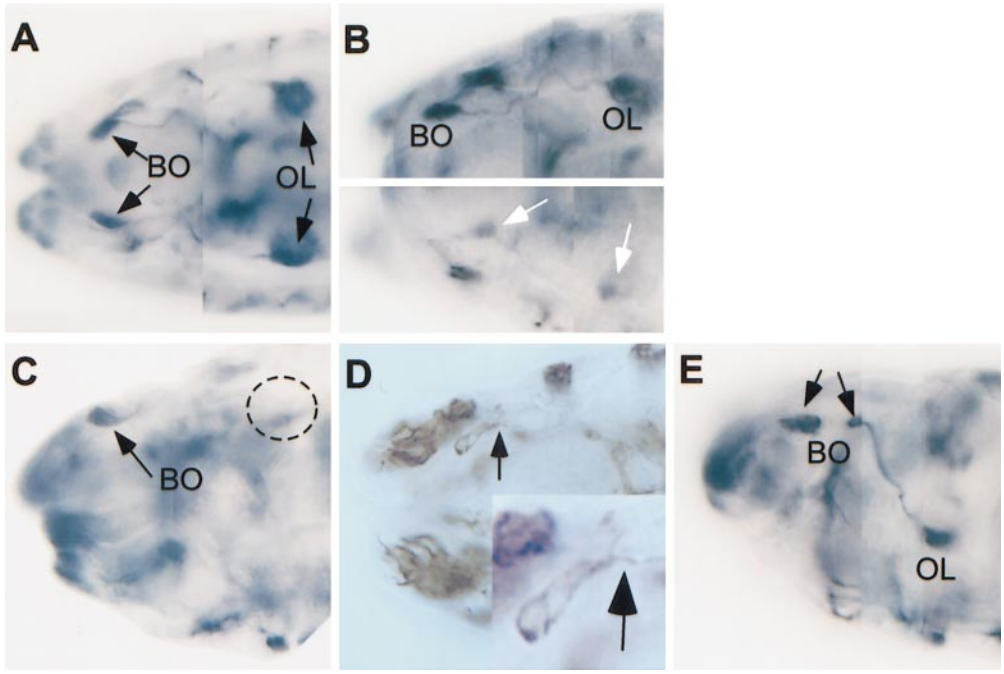

FIG. 5. Cell ablation by ricinA expression caused defects in the larval visual system. (A) Normal larval visual system consisting of the Bolwig's organ (BO) and optic lobe (OL) on both sides of the embryo was visualized by anti-FasII. (B to E) Ablation of cells in δ20 caused defects in the larval visual system. Four to six cells in δ20 were ablated by ricinA expression and the larval visual system was visualized by anti-FasII (B, C, E) or mAb 22C10 (D). In order to show the Bolwig's organ and optic lobe, images from multiple focal planes were combined. (B) The larval visual system on one side was missing (lower half). Faint expression of FasII was visible at the approximate location of the Bolwig's organ and optic lobe (white arrows). (C and D) Embryos with a truncated Bolwig's nerve. (C) FasII staining shows that this embryo was missing an optic lobe. The dashed-line circle indicates the expected position of the optic lobe. (D) mAb 22C10 labeling clearly showed that the Bolwig's nerve on one side was defasciculated (arrow) and had fewer than the normal number of photoreceptors as seen at higher magnification (inset). (E) An embryo with abnormal Bolwig's organ morphology. The Bolwig's organ was divided into two clusters (arrows) and the optic lobe appeared smaller than normal.

of the cell death-deficient mutant, *Df(3)H99*, referred to as *H99* (Abbott and Lengyel, 1991; White *et al.*, 1994; Grether *et al.*, 1995). The larval visual system in homozygous *H99* embryos was visualized in order to study the role of cell death in larval visual system development. In *H99* mutant embryos, head morphogenesis stalled such that when the abdomen appeared to complete embryogenesis, the head resembled that of a stage 13/14 embryo. PNS structures were differentiated in the head as evidenced by mAb 22C10, but the overall organization of these structures was far from normal. The Bolwig's organ was easily identified by its morphology in these embryos. Clustered photoreceptors with extending axons were found closely associated with the antennomaxillary complex. Although the Bolwig's organ roughly resembled the normal photoreceptor organ, there were many associated abnormalities. The most common defect was defasciculation of the Bolwig's nerve (Fig. 6A) and there was an increased number of photoreceptors in the Bolwig's organ, which sometimes formed a nice rosette shape (Fig. 6A), while others formed a large cluster of photoreceptors (data not shown).

δ20 Development in the Cell Death-Deficient Background

To determine the general development of δ20 in a cell death-deficient background, a large patch of δ20 cells in *UAS-lacZ; H99* embryos was activated. Since these embryos failed to carry out head involution, the distribution of δ20 progenitors was fairly similar to that of a stage 14 embryo even though the rest of the embryo had matured to stage 17 (Fig. 6B). The δ20 cells spread along the lateral surface reaching the dorsal part of the gnathal segments. A noticeable difference between *H99* and wild-type embryos was the extensive δ20 labeling on the dorsal surface of the *H99* embryo and at the ventral cluster, but the lateral cluster appeared normal (Fig. 6B, compared to Figs. 2C and 2D).

In order to determine if inhibition of cell death had a local effect on δ20 fates, the cell death inhibitor, p35, was selectively expressed in δ20 at gastrulation. Cell death inhibition of δ20 cells alone showed an expansion of dorsal surface epithelium (Fig. 6C). The defects in the *UAS-p35* embryos were mild compared to H99 embryos.

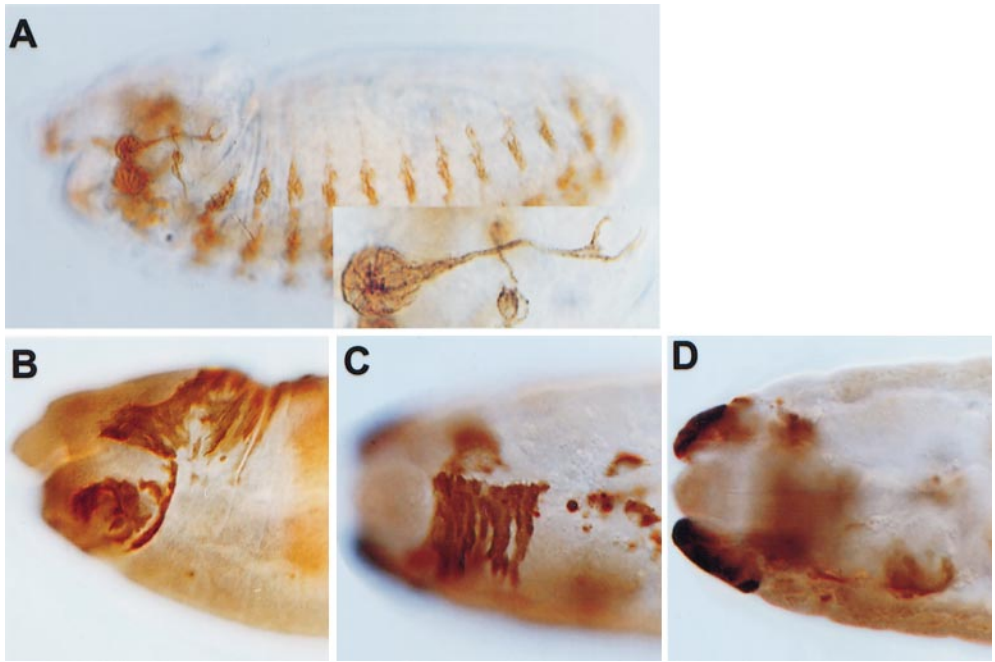

FIG. 6. Development of δ20 in the absence of cell death. (A) The PNS in a *H99* embryo was visualized with mAb 22C10. The Bolwig's organ was enlarged and the Bolwig's nerve was defasciculating (magnified view in the inset). (B) A lateral view of a *H99* embryo with δ20 labeling. The δ20 labeling area on the dorsal epithelium is expanded. (C and D) Dorsal views of a δ20 where cell death is inhibited by p35 expression in a *UAS-lacZ; UAS-p35* embryo. δ20 cells that were expressing p35 and β-galactosidase were visualized with an anti-β-galactosidase antibody.

All of the expected structures had a mostly normal location and arrangement, albeit they appeared to have extra cells (Fig. 6D). Some cell debris was still present in these embryos (Fig. 6C). This maybe be due to either insufficient p35 expression to inhibit cell death in all of the photoactivated cells or cells that were fated to die being removed from the epithelium by p35-independent processes.

DISCUSSION

Development of δ20

The development of δ20 is a good example of the extremely dynamic nature of procephalic morphogenesis. We found that δ20 cells that originated on the dorsal surface at gastrulation moved laterally and ventrally and ultimately spread along the dorsolateral surface to give rise to various ectodermal cell types throughout the head. It was surprising that fewer than a dozen cells gave rise to so many different structures. The location of these cells corresponded to the dorsal ridge, which is known to slide across the dorsal surface and create the dorsal pouch. In addition to the cells in the dorsal pouch, δ20 cells also were found at the anterior tip of the embryo forming sensory organs and nerves of the head peripheral nervous system. The peripheral nervous system has been shown to differentiate from the surface ectoderm (Hartenstein and Campos-Ortega, 1985; Technau and Campos-Ortega, 1985; Hartenstein, 1988). The sensory organs stay on the surface while their axons project into a distinct area of CNS. There are more than a dozen head sensory organs and some of them are assembled into a large sensory complex that can be identified by their location and distinct morphology (Jurgens *et al.*, 1986; Hartenstein, 1988; Schmidt-Ott *et al.*, 1994). Based on the morphology and labeling with mAb 22C10, we found that the larval photoreceptor organ, the Bolwig's organ, also derives from δ20.

Origin of the Larval Visual System

The shared origin of the larval photoreceptor organ and the optic lobe is not surprising since a previous study showed that the Bolwig's organ derives from the ventral part of the optic lobe invagination at stage 12 (Green *et al.*, 1993). However, it was unexpected that these structures originated from δ20 on the dorsal surface since the placode for the larval visual system was mapped to the dorsal lateral head region (Campos-Ortega and Hartenstein, 1985; Jurgens *et al.*, 1986; Green *et al.*, 1993). Moreover, by photoactivating a small number of cells at early gastrulation, we found that photoreceptors and optic lobe cells derive from a few

adjacent cells in the center of δ20. The results from the single-cell photoactivation experiments of δ20 suggest that the 12 photoreceptor cells originate from more than 1 δ20 cell and they share a common origin with the optic lobe precursors since single-cell photoactivation in the center of δ20 produced marked clones of photoreceptor cells that were always associated with optic lobe cells, but only a fraction of the 12 photoreceptor cells were derived from a single marked cell. We propose the following model: at gastrulation there is a small cluster of about 4 cells in the center of δ20 that are specified to become the photoreceptors and optic lobe, as well as part of the eye–antennal disc. It is very surprising that at the beginning of gastrulation, the cell fate boundary is already established in such a small area. The fate within this subdomain is specified at gastrulation but the final fate is probably not determined until later in development. Before starting the optic lobe invagination at stage 12, these cells have undergone four postblastoderm mitosis and form a field of optic lobe and photoreceptor precursors on the dorsal lateral part of the head. The final decision between optic lobe and photoreceptor cells may be determined by the local environment, such as the location of each cell within the field, rather than the strict lineage. An alternate explanation for the observed cluster of cells types arising from the center on δ20 is that the cells move to the appropriate positions to receive specific positional cues. This hypothesis would rely on limited cell mixing during head morphogenesis. Our observations indicate that there is extensive cell movement. Some of the cells remained clustered, while others moved in different directions. It is difficult to resolve the issue of early cell specification versus a positional cueing mechanism from these simple lineage marking experiments. More complex cell manipulations are required to discern between these two mechanisms.

The origin of the larval visual system in δ20 was also demonstrated by the fact that ablation of a small number of δ20 cells resulted in abnormal visual system development. When four to six cells were ablated by the selective expression of ricinA, some embryos showed developmental defects in the larval visual system. In some embryos, the Bolwig's nerve defasciculated before making the connection to the brain. This phenotype was similar to those observed in *disco* mutant embryos. *disco* mutants fail to make and maintain the accurate connection between the Bolwig's nerve and its target cells in the brain because of the failure in optic lobe differentiation (Steller *et al.*, 1987; Lee *et al.*, 1991; Campos *et al.*, 1995). In a few embryos, we could neither identify FasII-positive optic lobe nor Bolwig's nerve extending near the brain, suggesting that the defasciculation of the Bolwig's nerve may be due to the abnormality in the optic lobe caused by cell ablation. Although many Bolwig's organs were abnormal in shape and size and some optic lobes look smaller than normal, a surprisingly small number of ricinA embryos showed complete loss of the Bolwig's organ and the optic lobe. This may indicate that the embryos compensated for the loss of precursor cells in order to form a fairly normal larval visual system. The abundance of cell death in δ20 further supports the idea that there are excess cells that can be used to replace the ablated cells.

Many cells in δ20 died during embryogenesis as detected by the presence of cellular debris. Embryonic cell death which is an essential part of development is found throughout the embryo from the start of germ band retraction and is especially abundant in the head (Abrams *et al.*, 1993). Cells committed to die can be identified by the expression of *reaper* (*rpr*) (White *et al.*, 1994). *rpr* expression is seen as early as the onset of gastrulation and a region of strong expression can be found on the dorsal procephalic region roughly overlapping with the location of δ20 (Nassif *et al.*, 1998), supporting our observation that many of these cells are destined to die later. Cell death was not necessary for the differentiation of larval photoreceptor cells since cells in the cell-death-deficient embryos expressed PNS-specific antigens and extended axons. However, the structure of photoreceptor organ and the fasciculation of axons were abnormal in these embryos. Although some photoreceptor organs had more than 12 photoreceptor cells in the absence of cell death, a direct role of cell death in the development of larval visual system has yet to be determined. Most of the cell death originating in δ20 seemed to be on the dorsal surface since the inhibition of cell death resulted in the expansion of the dorsal epithelium.

Origin of the Eye–Antennal Disc

Cells in δ20 give rise to a large area of the dorsal pouch epithelium. Part of this epithelium is on the path of the Bolwig's nerve near the prospective site of the eye–antennal disc and the same area overlaps with the V-shaped pattern of *esg* expression which is a marker for the eye–antennal disc placode. Interestingly, in the single-cell-photoactivated embryos that showed the Bolwig's organ and optic lobe labeling, the same area of dorsal pouch was often marked. Thus, it seemed that precursors of the Bolwig's organ, optic lobe, and at least part of the eye–antennal disc all share the same origin within δ20.

Enhancer trap analysis suggested that the origin of the eye–antennal disc spanned a fairly large region across multiple head segments and these cells were brought together by cell death (Younossi-Hartenstein *et al.*, 1993). Since the area of the dorsal pouch deriving from δ20 does not overlap completely with the prospective eye–antennal disc, it is possible that other mitotic domains contribute to the disc development. In addition to δ20, δ18 is known to give rise to a part of the dorsal pouch, but it gives rise to cells in the center, away from the eye–antennal disc site. Although fates of dorsal and ventral head mitotic domains have been studied extensively (Cambridge, 1997; Namba, 1998; J. Mergliano and J. Minden, unpublished results), most lateral mitotic domains have yet to be studied. Further mapping of these head domains should clarify the multisegmental origin of the eye–antennal disc.

ACKNOWLEDGMENTS

J.M. is a Lucille P. Markey Scholar, and this work was supported in part by grants from the Lucille P. Markey Charitable Trust and by NIH Grant HD31642.

REFERENCES

Abbott, M. K., and Lengyel, J. A. (1991). Embryonic head involution and rotation of male terminalia require the *Drosophila* locus head involution defective. *Genetics* **129,** 783–789.

Abrams, J. M., White, K., Fessler, L. I., and Steller, H. (1993). Programmed cell death during *Drosophila* embryogenesis. *Development* **117,** 29–43.

Cambridge, S. B. (1997). "Studying Cell Fate in *Drosophila* Embryos with Photoactivated Gene Expression." Ph.D. thesis. Department of Biological Sciences, Carnegie Mellon University, Pittsburgh.

Cambridge, S. B., Davis, R. L., and Minden, J. S. (1997). *Drosophila* mitotic domain boundaries as cell fate boundaries. *Science* **277,** 825–828.

Campos, A. R., Lee, K. J., and Steller, H. (1995). Establishment of neuronal connectivity during development of the *Drosophila* larval visual system. *J. Neurobiol.* **28,** 313–329.

Campos-Ortega, J. A., and Hartenstein, V. (1985). "The Embryonic Development of *Drosophila melanogaster.*" Springer-Verlag, New York/Berlin/Heidelberg/Tokyo.

Cheyette, B. N., Green, P. J., Martin, K., Garren, H., Hartenstein, V., and Zipursky, S. L. (1994). The *Drosophila sine oculis* locus encodes a homeodomain-containing protein required for the development of the entire visual system. *Neuron* **12,** 977–996.

Endo, Y., and Tsuguri, K. (1988). The RNA N-glycosidase activity of ricin A-chain. The characteristics of the enzymatic activity of ricin A-chain with ribosomes and with rRNA. *J. Biol. Chem.* **263,** 8735–8739.

Foe, V. E. (1989). Mitotic domains reveal early commitment of cells in *Drosophila* embryos. *Development* **107,** 1–22.

Fujita, S. C., Zipursky, S. L., Benzer, S., Ferrus, A., and Shotwell, S. L. (1982). Monoclonal antibodies against the *Drosophila* nervous system. *Proc. Natl. Acad. Sci. USA* **79,** 7929–7933.

Fuse, N., Hirose, S., and Hayashi, S. (1996). Determination of wing cell fate by the *escargot* and *snail* genes in *Drosophila. Development* **122,** 1059–1067.

Goodman, C. S., Bastiani, M. J., Doe, C. Q., du, L. S., Helfand, S. L., Kuwada, J. Y., and Thomas, J. B. (1984). Cell recognition during neuronal development. *Science* **225,** 1271–1279.

Green, P., Hartenstein, A. Y., and Hartenstein, V. (1993). The embryonic development of the *Drosophila* visual system. *Cell Tissue Res.* **273,** 583–598.

Grether, M. E., Abrams, J. M., Agapite, J., White, K., and Steller, H. (1995). The head involution defective gene of *Drosophila melanogaster* functions in programmed cell death. *Genes Dev.* **9,** 1694–1708.

Halder, G., Callaerts, P., and Gehring, W. J. (1995). Induction of ectopic eyes by targeted expression of the *eyeless* gene in *Drosophila. Science* **267,** 1788–1792.

Hartenstein, V. (1988). Development of *Drosophila* larval sensory organs: Spatiotemporal pattern of sensory neurones, peripheral axonal pathways and sensilla differentiation. *Development* **102,** 869–886.

Hartenstein, V., and Campos-Ortega, J. A. (1985). Fate-mapping in wild-type *Drosophila melanogaster.* I. The spatio-temporal pattern of embryonic cell divisions. *Roux's Arch. Dev. Biol.* **194,** 181–195.

Hartenstein, V., Technau, G. M., and Campos-Ortega, J. A. (1985). Fate-mapping in wild-type *Drosophila melanogaster.* III. A fate map of the blastoderm. *Roux's Arch. Dev. Biol.* **194,** 213–216.

Heitzler, P., Coulson, D., Saenz-Robles, M. T., Ashburner, M., Roote, J., Simpson, P., and Gubb, D. (1993). Genetic and cytogenetic analysis of the 43A-E region containing the segment polarity gene *costa* and the cellular polarity genes *prickle* and *spiny-legs* in *Drosophila melanogaster. Genetics* **135,** 105–115.

Hidalgo, A., and Brand, A. H. (1997). Targeted neuronal ablation: The role of pioneer neurons in guidance and fasciculation in the CNS of *Drosophila. Development* **124,** 3253–3262.

Hidalgo, A., Urban, J., and Brand, A. H. (1995). Targeted ablation of glia disrupts axon tract formation in the *Drosophila* CNS. *Development* **121,** 3703–3712.

Jurgens, G., Lehmann, R., Schardin, M., and Nüsslein-Volhard, C. (1986). Segmental organization of the head in the embryo of *Drosophila melanogaster. Roux's Arch. Dev. Biol.* **195,** 359–377.

Lee, K. J., Freeman, M., and Steller, H. (1991). Expression of the *disconnected* gene during development of *Drosophila melanogaster. EMBO J.* **10,** 817–826.

Meinertzhagen, I. A., and Hanson, T. E. (1993). The development of the optic lobe. *In* "The Development of *Drosophila melanogaster*" (M. Bate and A. Martinez Arias, Eds.), pp. 1363–1492. Cold Spring Harbor Laboratory Press, New York.

Moffat, K. G., Gould, J. H., Smith, H. K., and O'Kane, C. J. (1992). Inducible cell ablation in *Drosophila* by cold-sensitive ricin A chain. *Development* **114,** 681–687.

Namba, R. (1998). "Embryonic Pattern Repair and Development of the Dorsal Procephalic Region in *Drosophila melanogaster* Embryos." Ph.D. thesis. Department of Biological Sciences, Carnegie Mellon University, Pittsburgh.

Namba, R., Pazdera, T. M., Cerrone, R. L., and Minden, J. S. (1997). *Drosophila* embryonic pattern repair: How embryos respond to *bicoid* dosage alteration. *Development* **124,** 1393–1403.

Nassif, C., Daniel, A., Lengyel, J. A., and Hartenstein, V. (1998). The role of morphogenetic cell death during *Drosophila* embryonic head development. *Dev. Biol.* **197,** 170–186.

Schmidt-Ott, U., Gonzalez-Gaitan, M., Jackle, H., and Technau, G. M. (1994). Number, identity, and sequence of the *Drosophila* head segments as revealed by neural elements and their deletion patterns in mutants. *Proc. Natl. Acad. Sci. USA* **91,** 8363–8367.

Schmucker, D., Jackle, H., and Gaul, U. (1997). Genetic analysis of the larval optic nerve projection in *Drosophila. Development* **124,** 937–948.

Schmucker, D., Su, A. L., Beermann, A., Jackle, H., and Jay, D. G. (1994). Chromophore-assisted laser inactivation of *patched* protein switches cell fate in the larval visual system of *Drosophila. Proc. Natl. Acad. Sci. USA* **91,** 2664–2668.

Schmucker, D., Taubert, H., and Jackle, H. (1992). Formation of the *Drosophila* larval photoreceptor organ and its neuronal differentiation require continuous *Kruppel* gene activity. *Neuron* **9,** 1025–1039.

Serikaku, M. A., and O'Tousa, J. E. (1994). *sine oculis* is a homeobox gene required for *Drosophila* visual system development. *Genetics* **138,** 1137–1150.

Sheng, G., Thouvenot, E., Schmucker, D., Wilson, D. S., and Desplan, C. (1997). Direct regulation of rhodopsin 1 by Pax-6/*eyeless* in *Drosophila:* Evidence for a conserved function in photoreceptors. *Genes Dev.* **11,** 1122–1131.

Steller, H., Fischbach, K. F., and Rubin, G. M. (1987). *disconnected:* A locus required for neuronal pathway formation in the visual system of *Drosophila. Cell* **50,** 1139–1153.

Struhl, G. (1981). A blastoderm fate map of compartments and segments of the *Drosophila* head. *Dev. Biol.* **84,** 386–396.

Technau, G. M., and Campos-Ortega, J. A. (1985). Fate-mapping in wild-type *Drosophila melanogaster.* II. Injections of horseradish peroxidase in cells of the early gastrula stage. *Roux's Arch. Dev. Biol.* **194,** 196–212.

Tix, S., Minden, J. S., and Technau, G. M. (1989). Pre-existing neuronal pathways in the developing optic lobes of *Drosophila. Development* **105,** 739–746.

Vincent, J.-P., and O'Farrell, P. H. (1992). The state of *engrailed* expression is not clonally transmitted during early *Drosophila* development. *Cell* **68,** 923–931.

White, K., Grether, M., Abrams, J., Young, L., Farrell, K., and Steller, H. (1994). Genetic control of programmed cell death in *Drosophila. Science* **264,** 677–683.

Younossi-Hartenstein, A., Tepass, U., and Hartenstein, V. (1993). Embryonic origin of the imaginal discs of the head of *Drosophila melanogaster. Roux's Arch. Dev. Biol.* **203,** 60–73.

Zipursky, S. L., Venkatesh, T. R., Teplow, D. B., and Benzer, S. (1984). Neuronal development in the *Drosophila* retina: Monoclonal antibodies as molecular probes. *Cell* **36,** 15–26.

Received for publication March 16, 1999
Revised May 18, 1999
Accepted May 18, 1999